

## Application of 2D inversion of magnetotelluric in exploration of hydrocarbon in south west of Iran

Shahrabi, M. A.<sup>1</sup>, Hafizi, M. K.<sup>2\*</sup>, Hashemi, H.<sup>3</sup> and Shahsavari, P.<sup>1</sup>

1. M. Sc. in Geophysics, Department of Earth Physics, Institute of Geophysics, University of Tehran, Iran

2. Professor, Department of Earth Physics, Institute of Geophysics, University of Tehran, Iran

3. Assistant Professor, Department of Earth Physics, Institute of Geophysics, University of Tehran, Iran

(Received: 22 Jun 2015, Accepted: 31 Jan 2016)

### Abstract

Since hydrocarbon sources have an important role in development of industry and technology, exploration of them has been lionized by human. The seismic reflection method is one of the most applicable investigative methods to identify the hydrocarbon reservoirs, but in some cases this method does not work well because of geology conditions and wave attenuation in depth. Thus, some exploration methods such as magnetotelluric can help us reach better results and lead to better interpretation of such reservoirs in compound with seismic methods. The Magnetotelluric (MT) method is suitable to map electrical resistivity in hydrocarbon explorations. This method has been widely used in exploration of conventional energy and also the renewable energy such as geothermal resources and a powerful tool to investigate different kinds of geological structures under the earth's surface. MT method usually focuses on the deeper geologic targets than the other EM methods. MT provides an excellent image of subsurface formations in the areas covered by high-velocity carbonate. The investigated area is located in southeastern part of the most prolific oil province of Iran, the Khuzestan in Dezful Embayment. Oil reservoirs of Iran have been contributed by Mesozoic and Cenozoic evaporated sediments. Multiple petroleum systems exist in the investigated area, since at least two proven source rocks exist within the area: The Kazhdumi and Pabdeh shale sediments. Three main groups of reservoirs are recognized in the Khuzestan basin: the Khami Group, the Bangestan Group and the Asmari Formation. All the three groups of reservoirs are recognized in investigated area with excellent fracture permeability and locally primary porosity. A formational interpretation of 2D inversion of MT data is used to demarcate hydrocarbon prospective formations underneath carbonated sediments of south west Iran. MT measurements are made in southwest Iran. The sites were distributed in two profiles of approximate SW-NE direction. Profiles are called P1 and P2, respectively. The MT experiment was carried out by deploying 63 sites with about 600 m spacing with 40 frequency values in seven decades and the period ranged 0.003-2000 (s). The dimensionality and the best geoelectrical strike estimation were carried out using tensor decomposition and phase tensor analysis. The ellipticity, phase tensor and skew angle are other measured parameters. NLCG inversion algorithm is used to inverse two MT data profiles. Both TE and TM modes with both MT polarizations were jointly inverted using the NLCG algorithm. The NLCG algorithm attempts to minimize an objective function that is the sum of the normalized data misfits and the smoothness of the model. The obtained MT sections show three anticlines underground. Seh Qanat anticline is the most important one in the investigated area. The lithological log of Seh Qanat Deep-1 (SQD-1) borehole is applied to interpret MT sections. This borehole has been drilled on Seh Qanat Anticline with total depth of 2876 meters. It could be detected a boundary of Asmari formation that is the primary shallow oil target in the investigated area. Other formations such as Sarvak, potentially are reservoir of hydrocarbon resources.

**Keywords:** Formational interpretation, Hydrocarbon resources, Magnetotelluric, NLCG Algorithm, 2D inversion.

### 1. Introduction

Magnetotelluric (MT) surveys could be considered as a strong tool to investigate various kinds of deep structures on the earth because of its large depth of penetration capability. This method has been widely used in exploration of conventional energy

(e.g. oil and gas) and also the renewable energy such as geothermal resources (Goldstein, 1988; Key et al., 2006; Orange, 1989). This method is also a powerful tool to investigate different kinds of geological structures under the earth's surface. MT

\*Corresponding author:

E-mail: hafizi@ut.ac.ir

method usually focuses on the deeper geologic targets than the other EM methods, though, complementary high-frequency data from audio-frequency MT (AMT) could be taken as part to probe the shallow structures and finally improve the resolution of reconstructed images (Lee et al., 2007). The MT method has been used to map sedimentary structures as an assistant to hydrocarbon exploration for several decades (e.g. Vozoff, 1972; Orange, 1989). The essence of the MT method is computation of electromagnetic earth impedance from measurements of orthogonal horizontal magnetic and electric fields on the surface. Estimates of impedance magnitude are transformed to an apparent resistivity and phase at various frequencies to allow investigation of electrical resistivity as a function of depth. Measured impedance in several locations allows investigation of resistivity as a function of horizontal position. The reliability and usefulness of the MT method has improved greatly the past few years as a result of progress in many areas. These include improvements in data-acquisition technology and technique (Nichols et al., 1988), the introduction of a remote reference to decrease the bias associated with noise in the magnetic-field measurements (Gamble et al., 1979), robust response function estimation methods (Egbert and Booker, 1986), and improved 1-D, 2-D, and 3-D forward and inverse modeling codes (Wannamaker et al., 1986; Constable et al., 1987; Smith and Booker, 1991). Seismic method is the most applicable tool and high-performance method for hydrocarbon explorations. However, in some cases, it has been a very challenging task, because of its inherent weakness in eliminating the low-velocity structures (such as sediments) underlying a heterogeneous high-velocity layer (Azeez et al., 2011). Carbonates commonly pose difficulties for reflection surveys because of excessive reverberations that effectively mask reflections from structures beneath them. Similarly, salt structures contain entrained sediments that produce significant scattering and, in addition, have been strong reflecting vertical boundaries. As a result, ambiguities in the interpretation of seismic

reflection data often remain unsolved. Electrical resistivity provides consequential complementary information about these situations (Hoversten et al., 1998). As a consequence, the MT method represents an influential non seismic exploration tool, particularly for discovery surveys in the areas where the seismic reflection method has poor performance.

The MT method is suitable to map electrical resistivity in hydrocarbon explorations. It can provide an excellent image of subsurface formations down to depths of 1-10 (km) and depending upon the magnetometer features of investigation. The reconnaissance depth can be increased to hundreds of kilometers (Favetto et al., 2008). This technique is extremely useful in the areas covered with high-velocity carbonates.

In this study, a 2D analysis of magnetotelluric data of two profiles has been done to examine the electrical resistivity changes on constitutive carbonated formations. The area is covered mostly with Lower Miocene Gachsaran Formation and consists of thick layers of hard anhydrite with marl, clay and limestone interbeds (Fig. 1).

## **2. Tectonic framework and Petroleum geology of study area**

The Zagros mountain range is an Alpine-type orogeny created by the collision of the continental Arabian plate with the segments of the Eurasian margin during Mesozoic and Cenozoic time. Oceanic Arabian plate crust was subducted northward beneath Eurasia. The continent to continent collision has begun locally since late Eocene, and the convergence is still continuing today. A consequence of this collision is creation of a depositional basin (the Zagros foreland Basin) across the Arabian shelf, southwest the Zagros suture. This convergence led to deformation of the basin area. The result of this convergence is southwest verging reverse faults and impressive whale back folding essentially parallel to the suture and dominant on the surface topography. This section has been involved in the subsequent folding in south western Iran (Rezaii, 2011; Motiei, 2010; Sahabi, 2012).

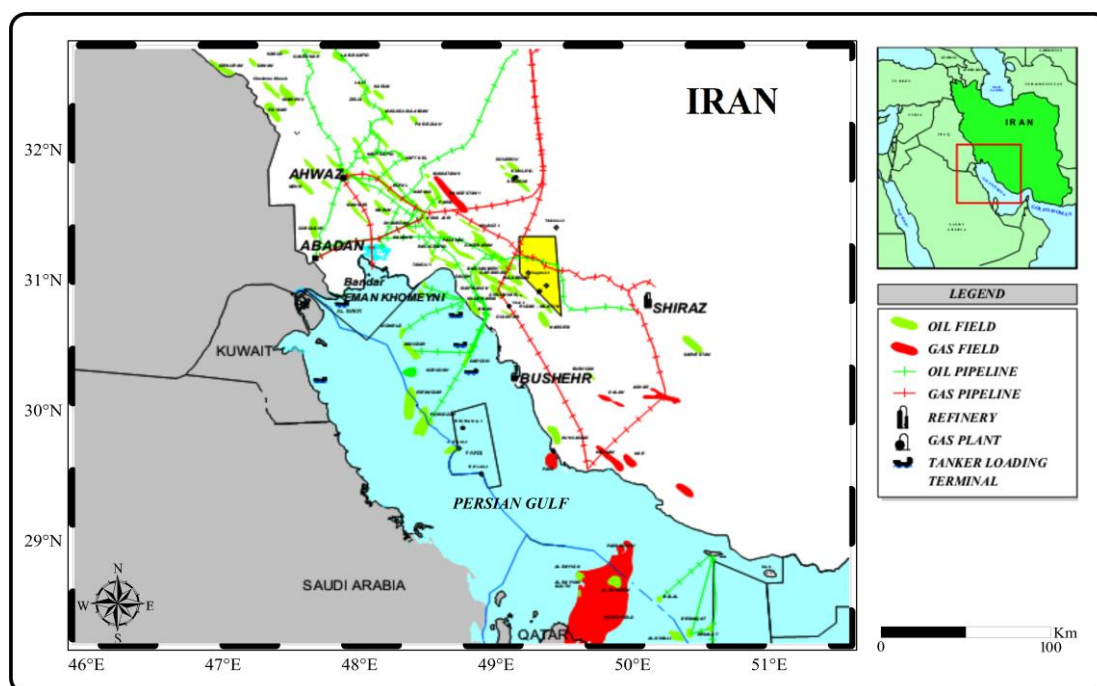


Fig. 1. Position of the study area in South West Iran (yellow rectangle)

The Zagros foreland basin contains a number of super-giant fields in high-amplitude structures created by the Neogene convergence. The studies on the hydrocarbon habitats of the fields of the basin have shown that all oil (and presumably gas) reserves have been sourced from stratigraphic levels predating the late Eocene. Hence, understanding the origin of the hydrocarbons trapped in the Zagros basin requires synthesis of the tectonics that has been beginning since late Proterozoic (Rezaii, 2011; Motiei, 2010; Sahabi, 2012).

The study area is located in southeastern part of the most prolific oil province of Iran, the Khuzestan in Dezful Embayment (Fig. 1). Multiple petroleum systems exist in the study area, since at least two proven source rocks exist within the area: The Kazhdumi and Pabdeh shale sediments. Three main groups of reservoirs are recognized in the Khuzestan basin: the Khami Group, the Bangestan Group and the Asmari Formation. All the three groups of reservoirs are recognized in the area with excellent fracture permeability and locally primary porosity (Rezaii, 2011; Motiei, 2010; Sahabi, 2012).

The Jurassic to Early Cretaceous Khami

Group is consisted of massive limestones and dolomites. These carbonates are extended in the whole Khuzestan. In Southeast of Khuzestan two main reservoir intervals include limestones of both Daryan and Fahlyan formations. The seals are the Kazhdumi and Gadvan shales. Traps are mainly anticlines which are frequently very different in shape and position from the corresponding anticlines at the surface (Rezaii, 2011; Motiei, 2010; Sahabi, 2012).

Bangestan Group has been created in mid late cretaceous. The main reservoir intervals are Sarvak and Ilam limestones. The Sarvak Formation consisted of high-energy limestones was deposited initially on the margins with high porosity and medium to high permeability. The shales of the formation provide the seal. Traps are classic anticlines often asymmetric, with a steep southwestern flank (Rezaii, 2011; Motiei, 2010; Sahabi, 2012).

The oligo-Miosene shallow marine Asmari reservoir is the most important formation in the Zagros fold belt and is capped by the Gachsaran evaporates. These provide an excellent seal with thick, high-energy carbonates (Rezaii, 2011; Motiei, 2010; Sahabi, 2012).

### 3. An overview of magnetotelluric method

The magnetotelluric (MT) method is a passive electromagnetic technique that uses the natural electromagnetic field variations to image the sub-surface electrical resistivity structures (Cagniard, 1953; Vozoff, 1991). The sources of the MT signals are the world-wide lightning activities and the Earth's magnetosphere. The lateral and vertical variations in Earth's sub-surface resistivity are measured by the simultaneous recording of the natural electric and magnetic-field fluctuations at the Earth's surface. The linear relationship between the horizontal components of electric (E) and magnetic (H) fields on the surface of the Earth can be written as,

$$E_x = Z_{xx}H_x + Z_{xy}H_y \quad (1)$$

$$E_y = Z_{yx}H_x + Z_{yy}H_y \quad (2)$$

where,  $x$  and  $y$  denotes the horizontal impedance tensor components. For two-dimensional earth structure, in which resistivity is invariant in one horizontal direction; the diagonal terms will be zero if the electromagnetic fields are defined in a coordinate system orthogonal to the strike of the structure. In such a case, the impedance component for the electric field parallel to strike (transverse electric (TE) mode) will be different from the component with the electric field perpendicular to the strike (transverse magnetic (TM) mode). If the impedance is measured in an arbitrary orientation, the angle (electric strike) required to rotate the measurements to deduce the TE and TM mode impedances can be obtained from the analysis of measured impedance tensor (Groom and Bailey, 1989).

The MT data is usually presented as apparent resistivity ( $\rho$ ) and phase ( $\varphi$ ) values. The impedance tensor, a complex magnitude, was rotated into principal directions and then converted into apparent resistivity and phase. It can be determined using the following relations:

$$\rho_{ij} = \frac{1}{2\pi f \mu} |Z_{ij}|^2 ; \quad (3)$$

$$Z_{ij} = \frac{E_{ij}}{H_{ij}} \quad (4)$$

$$\varphi_{ij} = \arctan\left(\frac{\text{Im}(Z_{ij})}{\text{Re}(Z_{ij})}\right) \quad (5)$$

where  $f$  is the frequency of the signal and  $\mu = 4\pi \times 10^{-7}$  is the magnetic permeability (Vozoff, 1991). The depth of penetration of the electromagnetic signal (skin depth) is a function of the electrical resistivity of the Earth ( $\rho$ ) and the frequency ( $f$ ) of investigation. It is defined as:

$$\delta = 503 \sqrt{\frac{\rho}{f}} \quad (6)$$

It could be seen that the penetration depth of the electromagnetic fields can increase with period (reciprocal of frequency) and resistivity. The broad range of frequency (1000-0.0001 Hz) used in MT can scan the sub-surface from few tens of meters to hundreds of kilometers. Generally, inverse modeling of a number of sites and a range of frequencies is employed simultaneously to extract the subsurface resistivity structure embodied in the MT data. Due to the depths involved, MT is a very convenient technique to image the resistivity distribution and characterizing the structures of hydrocarbon resources.

### 4. Data acquisition

MT measurements are made in southwest Iran. Total of the sites were distributed in two profiles of approximate SW-NE direction. Profiles are called P1 and P2, respectively. The MT experiment was carried out by deploying 63 sites with about 600 m spacing with 40 frequency values in seven decades and the period range of 0.003-2000 s. The relatively high number of frequencies applied for data gathering in each site is because of the increase of vertical resolution of the obtained resistivity images. At each point, horizontal electric and magnetic-field components and the vertical magnetic component were measured. The only borehole in the investigated area is SQD-1 borehole located in the middle of profile P1 with total depth of 2876 m from the surface. The magnetotelluric profiles have been interpreted in this study, the location of the profiles and situation of drilled borehole has been shown in Figure 2.

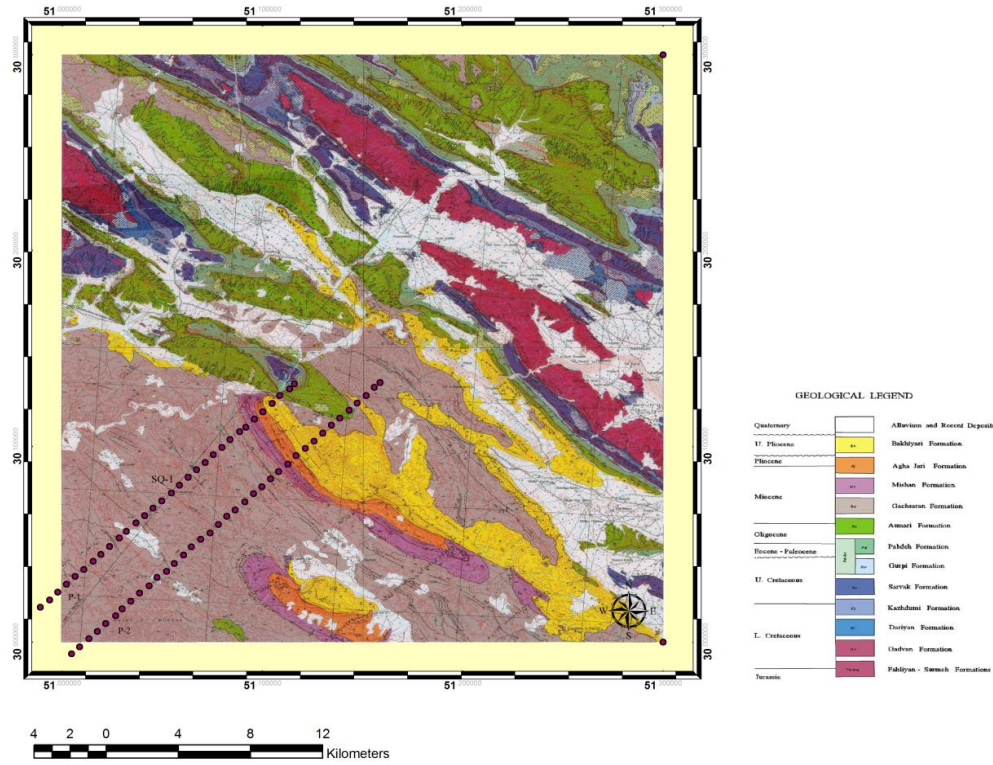


Fig. 2. Location of magnetotelluric sites and SQ-1 borehole on geological map of the study area

## 5. Data processing and inversion

The dimensionality and the best geoelectrical strike estimation were studied using tensor decomposition and phase tensor analysis (Caldwell et al., 2004). Decomposing impedance tensors  $Z$  into real (X) and imaginary (Y) parts as

$$Z = X + iY \quad (7)$$

X and Y define the phase tensor  $\varphi$  as

$$\varphi = X^{-1}Y \quad (8)$$

The phase tensor is graphically represented by an ellipse. An invariant parameter of this tensor is the skew angle. Swift (1967) initially introduced this parameter to evaluate the dimensionality of regional electrical structure and it was defined as:

$$S = \text{Arc tan}((\varphi_{ij} - \varphi_{ji})/(\varphi_{ii} + \varphi_{jj})) \quad (9)$$

The phase tensor skew angle determines whether the 2D structure approximation is valid when its absolute value is less than 1.5 (Bibby et al., 2005). Correspondent minimal amplitude azimuths for all sites of P1 and P2 profiles at periods 0.003–20,000 s are summarized in rose diagrams shown in Figure 3. According to these diagrams, a

common strike was selected for both P1 and P2 profiles perpendicular to dominant directions in these diagrams. The observed apparent resistivity and phase curves of MT sites of the first, middle and end of two profiles are shown in two upper parts of the Figures 4 and 5 as the examples. It seems that the curves of XY component are more stable and smooth than those of YX component. The data over the period ranged from 0.003 s to 100 s are less contaminated by noise.

Another invariant, called ellipticity is defined as:

$$\lambda = ((\varphi_{\max} - \varphi_{\min})/(\varphi_{\max} + \varphi_{\min})) \quad (10)$$

This parameter determines that the structure approximates to 1D when it takes values smaller than 0.1. These parameters were calculated at all the sites.

Two lower parts of Figures 5 and 6 show the ellipticity, phase tensor and skew angle (orientation of the major axis which coincides with the strike in the 2D situation) at corresponding site. This can be considered representative of the average behavior of all sites. Skew angle is smaller than 0.5 for all periods, and ellipticity is smaller than 0.1 for the periods less than 1s.

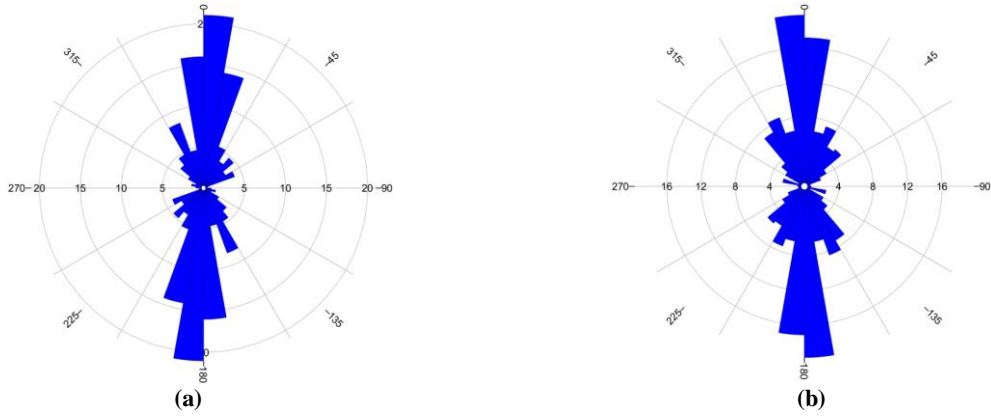


**Fig. 3.** The rose diagram plot representing all the site strike analysis results of P1 and P2 profiles of the MT data in period range of 0.003- 2000 s.

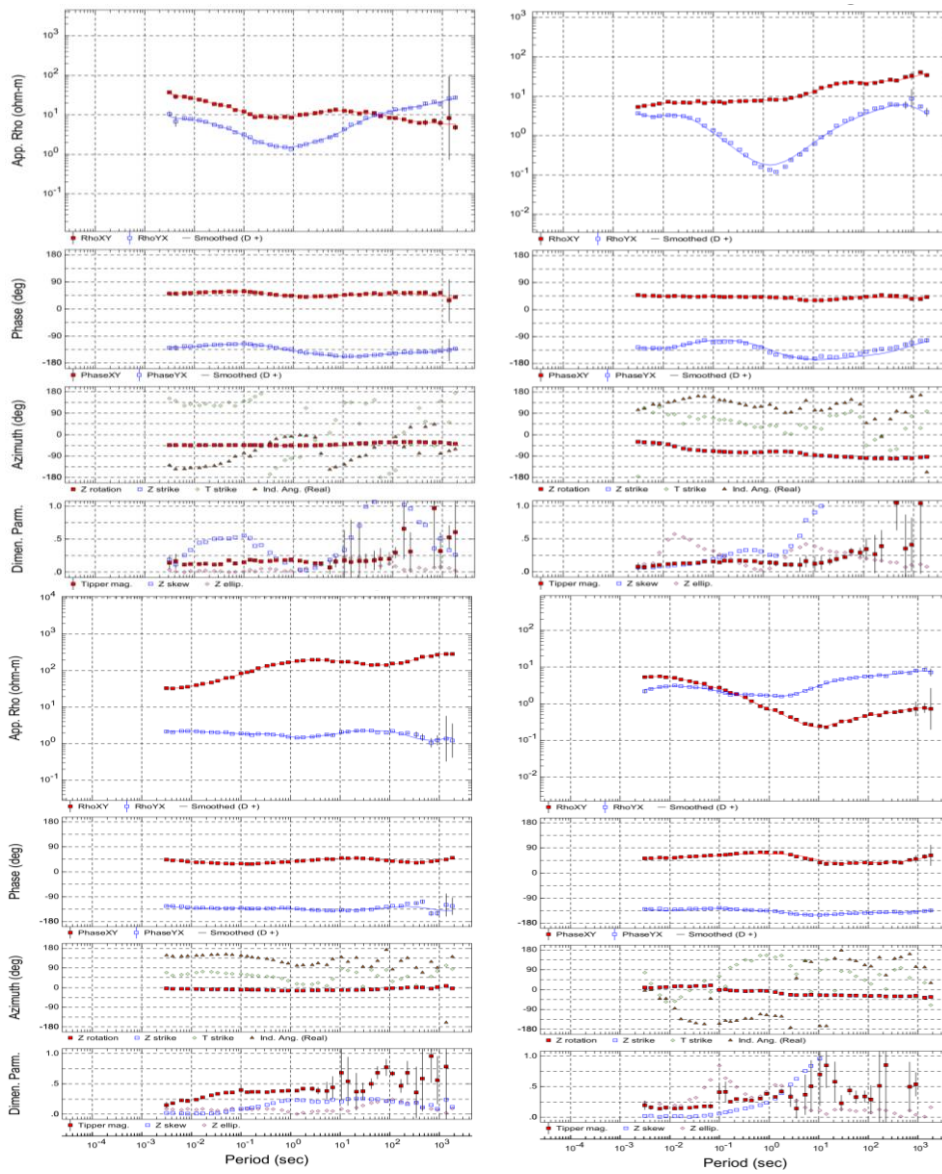


**Fig. 4.** The fit between the observed and calculated data for four representative sites is selected from different parts of P-1 profile. For each site two upper parts are: TE for apparent resistivity and phase (red), TM for apparent resistivity and phase (blue), solid lines for calculated data and squares for the observed data; and two lower parts are the variation of azimuth and dimension parameters for the period: Z strike, T strike and induction angle (azimuth parm) and Tipper magnitude, skew and ellipticity (dimen parm).

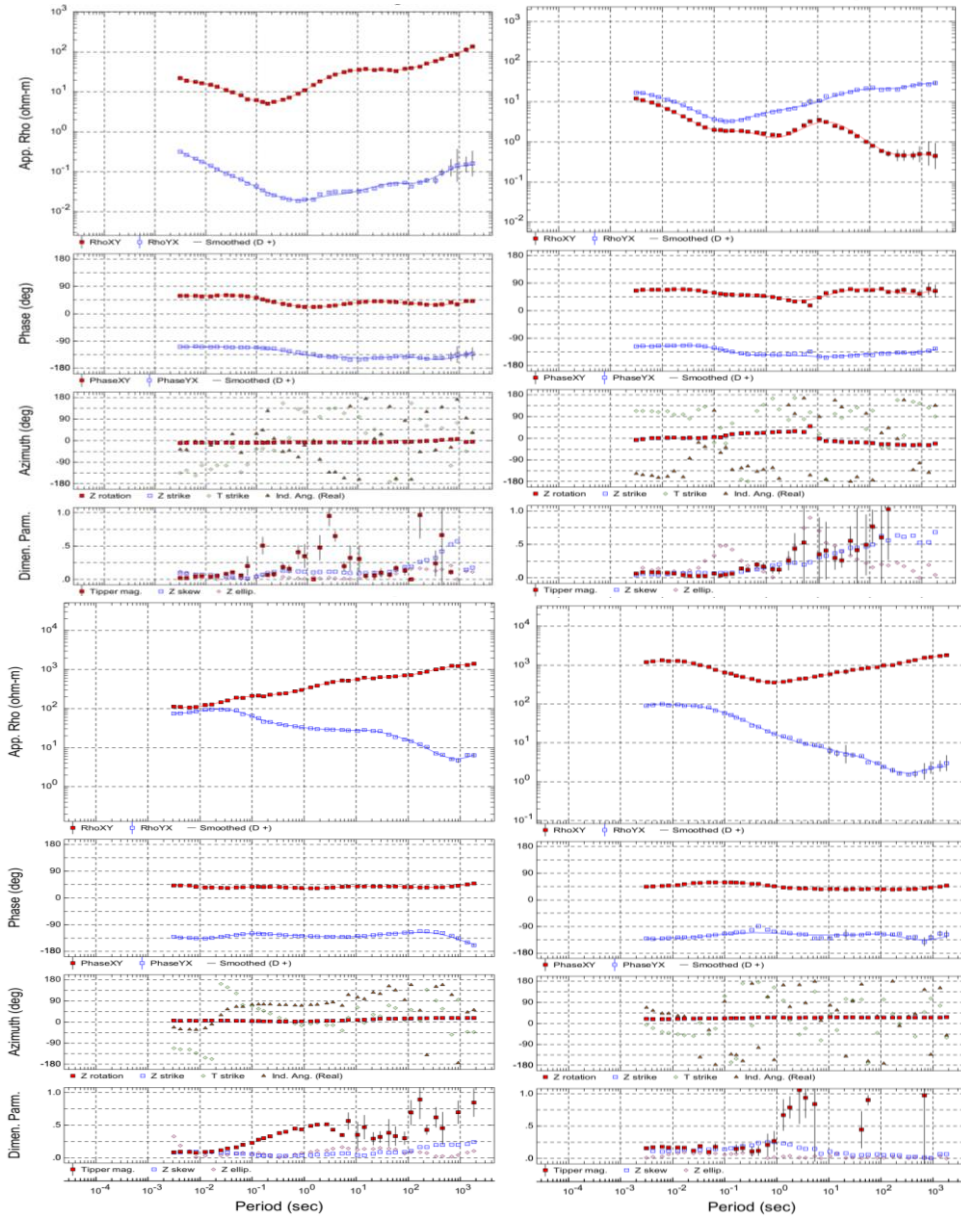


**Fig. 5.** The fit between observed and calculated data for four representative sites selected from different parts of P-2 profile. For each site two upper parts are: TE for apparent resistivity and phase (red), TM for apparent resistivity and phase (blue), solid lines for calculated data and squares for the observed data; and two lower parts are the variation of azimuth and dimension parameters for the period: Z strike, T strike and induction angle (azimuth parm) and Tipper magnitude, skew and ellipticity (dimen parm).

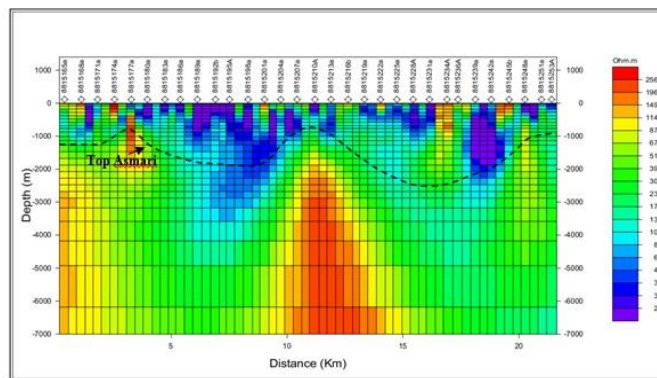


**Fig. 6.** Resistivity model result of MT inversion; mesh model for profile P-1, (22 km long, 7 km deep) in the scale 2-256 ohm.m.

## 6. Inversion

Apparent resistivities and impedance phases decomposed into strike direction were used to obtain the models. Noise of all data were almost zero for short periods and a little noisy for the last decade in some sites. Both TE and TM modes with both MT polarizations were jointly inverted using the NLCG algorithm of Rodi and Mackie (2001). The NLCG algorithm attempts to minimize an objective function as the sum of the normalized data misfits and the smoothness of the model. The tradeoff between data misfits and model smoothness is controlled by the regularization parameter  $\tau$ . Different values of  $\tau$  were applied and inversion process was done by this values and the best MT model was obtained by the value of  $\tau=4$ . In this paper, roughness is defined as the integral gradient of the model, assuming a standard Laplacian grid. The standard Laplacian may produce a rougher-looking model, but the definition of smoothness is consistent with the model dimensions. The scale factor for roughness penalty  $\beta$ , is set to 1.0 and  $\alpha$  is set to 1.0 for two profiles. Taking  $\beta=1$  means that the penalty on horizontal roughness increases with depth at the same rate as the vertical roughness. This means that the model will be smoother in both the vertical and horizontal directions as depth increases. Static shift was corrected by fitting in the inversion processing after obtaining a good fitting of the data with the assumption that static shifts are due to a zero-mean Gaussian process (Sasaki, 2004; Ogawa and Uchida, 1996).

The depth and lithology obtained in P1 is in agreement with the obtained information of the well drilled in the middle of this profile. Because two profiles are almost close to each other, information of this well could be distributed to the two profiles. For all the models, detail interpretation is described in next section.

## 7. Discussions

The obtained MT inversion models of P-1 and P-2 profiles were represented in Figures 6 and 8, respectively. Furthermore, pseudo sections of apparent resistivity and phase data of each profile were represented

in Figures 7 and 9. Three anticlines exist in the study area: Dara, Seh-Qanat and Murd Anticlines. In P-1 profile the Dara anticline nose is under station 8815177A and Seh-Qanat is located under 8815213a station. Murd anticline is not visible completely in P-1 profile, but the south flank of it, is located at the end of the profile. In P-2 profile, the Dara anticline is under station 8816203A and Seh-Qanat anticline nose is located under station 8815245a and Murd anticline is located under station 8816278.

Gachsaran Formation consists of alternations of evaporated sediments like anhydrites, marls and thin-bedded limestones. Lower part of the Gachsaran Formation known as 'Cap Rock' is composed of anhydrite and marl. Dolomitization is the important process that affected the Cap Rock. The upper part of this Formation consists of a thick salt layer. The resistivity range of Gachsaran Formation is 2-24 ohm.m. In P-1 profile the Gachsaran Formation has been spread all the area except in the stations of 8815236 to 8815248 that is thrust over Mishan Formation. This overlay explains abrupt lateral resistivity change at here. The structural high at this station may reflect Asmari Formation brought up along this fault. At the end of P-2 profile below the Mishan, the top resistor is interpreted as the top Asmari situated on the footwall of the main reverse fault south of the Murd Anticline. Top Asmari as the primary target at this area is located below the Gachsaran Formation and starts at 24 ohm.m resistivity value. The Upper Asmari consists of dolomite; in evaporate, with thin levels of anhydrite. Middle and lower Asmari are belonged to early Miocene and Oligocene where consisted of the dolomite cemented by anhydrite and limestone at the end of the Formation. Generally, increase in depth is corresponding with decrease in dolomite on Asmari Formation.

Resistivity range of 51-115 ohm.m belongs to Pabdeh and Gurpi Formations that consists of shale and marl at the top and fine marl, shale and a little marly limestone at the bottom. The Gurpi Formation is generally considered as a seal for the Upper Cretaceous reservoirs or as a potential source rock. But in the area, the

Gurpi is not buried deep enough to generate hydrocarbons. These two formations belong to Eocene and Oligocene. Other formations in the study area are Sarvak, Kazhdumi and Daryan Formations with resistivity range of 115- 256 ohm.m. Sarvak Formation belongs to Albian and Cenomanian geology time.

Kazhdumi and Daryan formations

consist of calcareous marl/shale and clay limestone. Resistivity values higher than the 180 ohm.m could be given to these formations.

Fahlyan Formation is comprised of oolite limestone. This formation is a member of Khami group and isocline with Surmeh formation from the bottom.

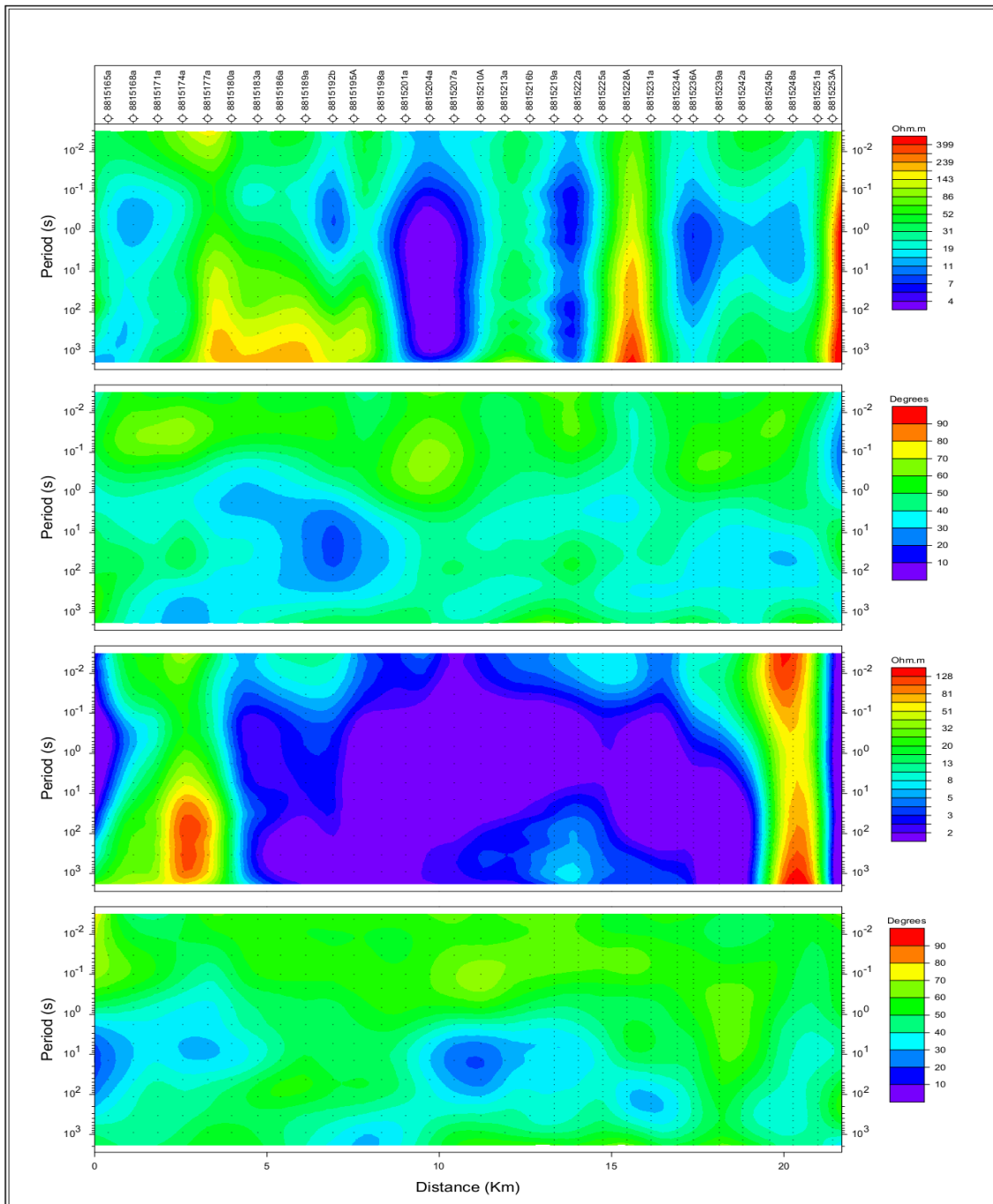


Fig. 7. Pseudo section data of resistivity and phase data for TE (two upper sections) and TM (two lower sections) modes of P-1 Profile.

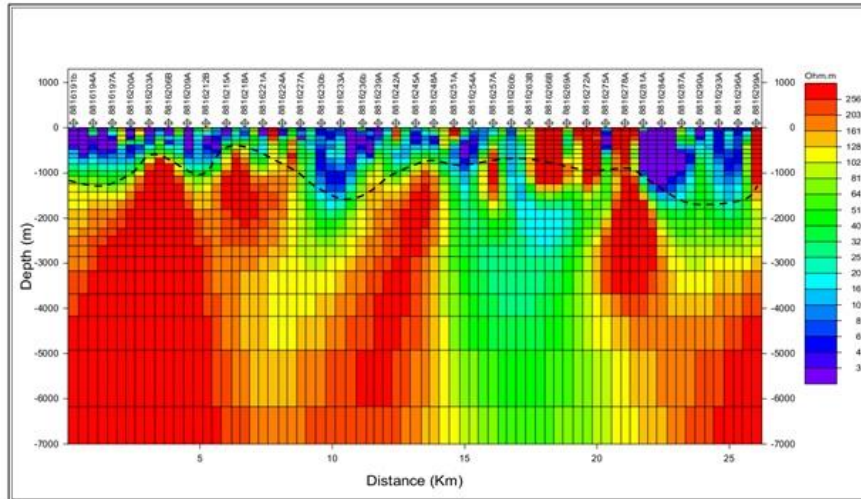


Fig. 8. Resistivity model result of MT inversion; mesh model for profile P-2, (26 km long, 7 km deep) in the scale 2-256 ohm.m.

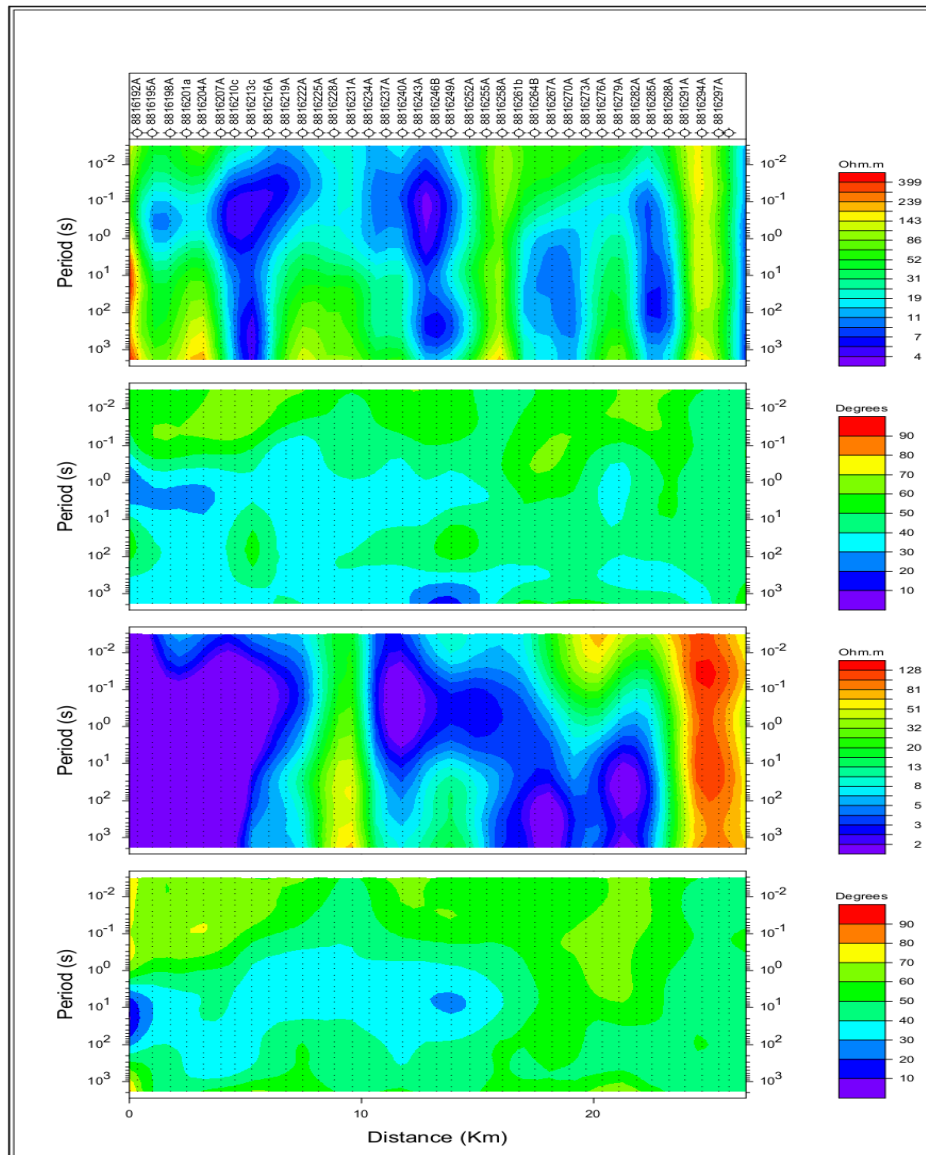


Fig. 9. Pseudo section data of resistivity and phase data for TE (two upper sections) and TM (two lower sections) modes of P-2 Profile.

## 8. Conclusions

In application of 2D magnetotelluric inversion in the study area, TM&TE modes are jointly inverted with a reasonable value of data misfit. The resistivity models could be compared with each other and coincided with the known geology and drilling results of SQD-1 borehole. This means that the magnetotelluric method applied in the position prognosis is effective in concealed hydrocarbon resources.

It could be concluded that MT study is a successful, economic and practical reconnaissance tool to explore hydrocarbon prospective areas. In salty evaporated sediment covered regions which seismic method faces with wave attenuation in depth the MT that could especially be a suitable superseded method.

## Acknowledgments

We are grateful to NIOC exploration directorate that supported this study by sharing the MT information. We wish to thank also Mehrdad Darijani and Amir Ashtari for their support.

## References

- Azeez, K. K. A., Kumar, T. S., Basava, S. T., Harinarayana, and Dayal, A. M., 2011, Hydrocarbon prospects across Narmadae Tapti rift in Deccan trap, central India: inferences from integrated interpretation of magnetotelluric and geochemical prospecting studies, *J Marine and Petroleum Geology*, 28, 1073-1082.
- Cagniard, L., 1953, Basic theory of magnetotelluric method of geophysical prospecting, *Geophysics*, 18, 605-635.
- Caldwell, G. T., Bibby, M. and Brown, C., 2004, The magnetotelluric phase tensor, *Geo-phys. J. Int.*, 258, 457-469.
- Constable, S. C., Parker, R. L. and Constable, C. G., 1987, Occam's inversion: a practical algorithm for generating smooth models from EM sounding data, *Geophysics*, 52, 289-300.
- Egbert, G. D. and Booker, J. R., 1986, Robust estimation of geomagnetic transfer functions, *Geophys. J. R. Astr. Soc.*, 87, 173-194.
- Favetto, A., Pomposiello, M. C., López de Luchi, M. and Booker, J., 2008, 2D Magnetotelluric interpretation of the crust electrical resistivity across the Pampean Terrane Río de la Plata suture, in *Central Argentina, Tectonophysics*, 459, 54-65.
- Gamble, T. D., Goubau, W. M. and Clarke, J., 1979, Magnetotellurics with a remote magnetic reference, *Geophysics*, 44, 53-68.
- Goldstein, N. E., 1988, Subregional and detailed exploration for geothermal hydrothermal resources, *Geotherm. Sci. Tech.*, 1, 303-431.
- Groom, R. W. and Bailey, R. C., 1989, Decomposition of magnetotelluric impedance tensors in the presence of local three-dimensional galvanic distortion, *Journal of Geophysical Research* 94, 1913-1925.
- Lee, T. J., Song, Y. and Uchida, T., 2007, Three-dimensional magnetotelluric surveys for geothermal development in Pohang, Korea, *Explor. Geophys.*, 60, 89-97.
- Moteie, H., 2010, Petroleum geology of Iran, Arian Publications, pp. 978-964-91038-3-9.
- Nichols, E. A., Morrison, H. F. and Clarke, J., 1988, Signals and noise in measurements of low-frequency geomagnetic fields, *J. Geophys. Res.*, 93, 743-754.
- Orange, A.S., 1989, Magnetotelluric exploration for hydrocarbons, *Proc. IEEE*, 77, 287-317.
- Ogawa, Y. and Uchida, T., 1996, A two-dimensional magnetotelluric inversion assuming Gaussian static shift: *Geophys. J. Int.*, 126, 69-76.
- Rezaie, M. R., 2011, Petroleum geology of Iran, Alavi Publications, pp. 978-964-310-409-2.
- Rodi, W., Mackie, R. L., 2001, Nonlinear conjugate gradients algorithm for 2-D magnetotelluric inversion. *Geophysics*, 66, 174-187.
- Sahabi, F., 2012, Petroleum geology, University of Tehran, pp. 978-964-03-3790-5.
- Sasaki, Y., 2004, Three-dimensional inversion of static-shifted magnetotelluric data, *Earth Planets Space*, 56, 239-248.
- Smith, J. T. and Booker, J. R., 1991, Rapid

- inversion of two- and three-dimensional magnetotelluric data, *J. Geophys. Res.*, 96, 3905-3922.
- Vozoff, K., 1991, The magnetotelluric method, in *Electromagnetic Methods in Applied Geophysics*, 2, 641-711.
- Wannamaker, P. E., Stodt, J. A. and Rijo, L., 1986, A stable finite element solution for two-dimensional magnetotelluric modelling, *Geophys. J. Roy. Astr. Soc.*, 88, 277-296.